



Reconstruction of wideband reflectivity densities by wavelet transforms

Stephan Dahlke *, Peter Maass ** and Gerd Teschke ***

Fachbereich 3, Universität Bremen, Postfach 33 04 40, 28334 Bremen, Germany
E-mail: dahlke@math.uni-bremen.de

Received 6 August 2001; accepted 7 December 2001

Communicated by C.A. Micchelli

This paper is concerned with reconstruction problems arising in the context of radar signal analysis. The goal in radar is to obtain information about objects by emitting certain signals and analyzing the reflected echoes. In this paper, we shall focus on the general wideband model for radar echoes and on the case of continuously distributed objects D (reflectivity density). In this case, the echo is given by an inverse wavelet transform of the density D where the role of the analyzing wavelet is played by the transmitted signal. However, the null space of an inverse wavelet transform is nontrivial, it is described by the corresponding reproducing kernel. Following the approach of Naparst [14] and Rebolla-Neira et al. [16], we suggest to treat this problem by transmitting not just one signal but a family of signals. Indeed, a reconstruction formula for one- and 2-dimensional reflectivity densities can be derived, provided that the set of outgoing signals forms an orthogonal basis or – more general – a frame. We also present some rigorous error estimates for these reconstruction formulas. The theoretical results are confirmed by some numerical examples.

Keywords: radar, reflectivity density, wideband regime, frames, Jackson-type estimates, wavelets

AMS subject classification: 41A25, 42C15, 42C40, 65J22

1. Introduction

In recent years, wavelet analysis has been successfully applied to many problems in signal analysis and image processing as well as in numerical analysis. Moreover, since the pioneering work of Naparst [14,15], it is well known that the specific features of wavelets can also be efficiently used for treating reconstruction problems in the context

* The work of this author has been partially supported by Deutsche Forschungsgemeinschaft, Grants Da 117/13-1, Da 360/4-1.

** The work of this author has been partially supported by Deutsche Forschungsgemeinschaft, Grant Ma 1657/6-1.

*** The work of this author has been partially supported by BMBF, Grant 3MAM1HB.

of radar signal analysis. Related approaches to radar applications have been investigated by [7,12,13], more recently the original approach of Naparst has been extended by [16].

The basic radar problem seeks to gain information about an object by analyzing the waves reflected from it. To describe this simplified setting, let us first assume that the object under consideration can be described as a point, moving at a constant velocity v towards or away from a given source. The distance between object and source at time $t = 0$ is denoted by R . The emitted signal is denoted by $h(t)$; then the *wideband model* for the received echo $f(t)$ is given by

$$f(t) = \sqrt{|s|}h(s(t - \tau)), \quad (1.1)$$

where the *Doppler scale factor* s is obtained from the speed of light c and the object velocity v as

$$s = \frac{c - v}{c + v}, \quad (1.2)$$

and the delay τ is determined by the distance R between the object and the source as

$$\tau = \frac{2R}{c - v}. \quad (1.3)$$

The so-called Doppler coordinates (s, τ) are in one-to-one correspondence to the desired values v and R . The multiplicative factor $\sqrt{|s|}$ is chosen such that the energy is conserved, i.e., we assume a perfectly reflecting object. For further information, the reader is referred, e.g., to [8–10].

In the presence of many objects the total echo is modelled as the superposition of single echoes. More general, if we assume that we want to observe a reflecting continuum with varying reflectivity as described in Doppler coordinates by a *reflectivity density* $D(\tau, 1/s)$, then the total echo is given by

$$f(t) = \int_{\mathbb{R}} \int_{\mathbb{R} \setminus \{0\}} D(\tau, s) |s|^{-1/2} h\left(\frac{t - \tau}{s}\right) \frac{ds d\tau}{s^2}. \quad (1.4)$$

Consequently, the task is to reconstruct the density $D(\tau, s)$ from the received echo. To treat this problem, let us first remark that formula (1.4) can be reinterpreted in the context of wavelet analysis: in general, the *continuous wavelet transform* $W_\psi(F)$ of a function $F \in L_2(\mathbb{R})$ is given by

$$(W_\psi F)(a, b) := \int_{\mathbb{R}} F(x) |a|^{-1/2} \overline{\psi\left(\frac{x - b}{a}\right)} dx. \quad (1.5)$$

This transformation is well-defined, provided that the analyzing wavelet ψ satisfies the admissibility condition

$$C_\psi = \int_{\mathbb{R}} \frac{|\hat{\psi}(\xi)|^2}{|\xi|} d\xi < \infty. \quad (1.6)$$

The wavelet transform W_ψ is a multiple of isometry whose inverse is given by the adjoint wavelet transform

$$\begin{aligned} F(x) &= W_\psi^*(W_\psi F(a, b))(x) \\ &= \frac{1}{C_\psi} \int_{\mathbb{R}} \int_{\mathbb{R} \setminus \{0\}} (W_\psi F)(a, b) |a|^{-1/2} \psi\left(\frac{x-b}{a}\right) \frac{da}{a^2} db, \end{aligned} \quad (1.7)$$

see, e.g., [3,8,11] for details. Therefore a comparison of (1.7) with (1.4) yields the well-known and basic identity which links wideband radar echoes to the wavelet analysis, see, e.g., [7,13,14]: the echo f is identical with the inverse wavelet transform of the searched reflectivity distribution D , where the transmitted signal h plays the role of the analyzing wavelet.

This suggests recovering D by computing the wavelet transform of the echo f :

$$D(\tau, s) := \frac{1}{C_h} [(W_h f)(\tau, s)]. \quad (1.8)$$

However, the null space \mathcal{N} of an inverse wavelet transform is nontrivial. Hence, by this procedure one can only recover the component of D which lies in the orthogonal complement of \mathcal{N} or, equivalently, one can recover the component of D in the range of the wavelet transform W_h .

To our knowledge, there exists no physical principle that guarantees that D is in fact contained in the range of W_h , so that (1.8) describes only one part of the desired density D . Inspired by these problems, Naparst [14,15] was the first one who suggested to transmit not just *one* signal, but a *family* of signals. In his fundamental work, Naparst primarily studied the case where the transmitted signals form an orthonormal basis. However, this assumption is very restrictive in practice. Therefore, quite recently, Rebollo-Neira et al. have generalized Naparst's approach to the case of transmitting a *frame* of signals, which is a much weaker restriction [16]. The present study is very much inspired by their results, however, we modify and generalize their approach in the following sense:

- rigorous error estimates in suitably weighted L_2 -spaces are given in section 3;
- a generalization to the multivariate case is discussed in section 4; this includes an inversion formula for a suitable subclass of 2D reflectivity distributions;
- numerical examples using orthogonal and biorthogonal wavelets confirm the theoretical results in section 5.

Moreover, the proof of the basic reconstruction formula in section 2 is significantly shorter as compared to the exposition in [16].

2. Basic reconstruction formulas

In general, the reflectivity distribution $D(\tau, s)$ cannot be reconstructed from the knowledge of a single echo. Following the approach of [14,16] we assume that echoes

$$f_m(t) = \int_{\mathbb{R}} \int_{\mathbb{R} \setminus \{0\}} D(\tau, s) |s|^{-1/2} h_m\left(\frac{t-\tau}{s}\right) \frac{ds d\tau}{s^2} \quad (2.1)$$

are available for a family of submitted signals $\{h_m\}_{m \in \mathbb{Z}}$. Naparst proved a reconstruction formula under the assumption that $\{h_m\}_{m \in \mathbb{Z}}$ forms an orthogonal basis. We follow the approach of Rebollo-Neira et al. and assume a weaker condition, namely, that $\{h_m\}_{m \in \mathbb{Z}}$ forms a frame in $L_2(\mathbb{R})$. The original proof in [16] is somewhat complicated and long, we will present a shorter proof using some standard Fourier techniques.

Let us briefly recall the notion of a frame. In general, a system $\{h_m\}_{m \in \mathbb{Z}}$ of functions is called a *frame* if there exist constants A and B , $0 < A \leq B < \infty$, such that

$$A \|F\|_{L_2(\mathbb{R})}^2 \leq \sum_{m \in \mathbb{Z}} |\langle F, h_m \rangle|^2 \leq B \|F\|_{L_2(\mathbb{R})}^2. \quad (2.2)$$

The numbers A, B are called *frame bounds*. Given a frame $\{h_m\}_{m \in \mathbb{Z}}$, one defines the *frame operator* T as

$$T(F) := \sum_{m \in \mathbb{Z}} \langle F, h_m \rangle h_m. \quad (2.3)$$

For later use, let us recall the following fundamental theorem which was proved in [5].

Theorem 2.1. Let $\{h_m\}_{m \in \mathbb{Z}}$ be a frame in $L_2(\mathbb{R})$. Then the following holds:

- (i) T is invertible and $B^{-1}I \leq T^{-1} \leq A^{-1}I$.
- (ii) $\{h^m\}_{m \in \mathbb{Z}}$, $h^m := T^{-1}h_m$ is a frame with bounds A^{-1} , B^{-1} , called the *dual frame* of $\{h_m\}_{m \in \mathbb{Z}}$.
- (iii) Every $F \in L_2(\mathbb{R})$ can be written as

$$F = \sum_{m \in \mathbb{Z}} \langle F, h^m \rangle h_m = \sum_{m \in \mathbb{Z}} \langle F, h_m \rangle h^m. \quad (2.4)$$

Furthermore, we need a result concerning the Fourier transform of frames.

Lemma 2.1. Let $\{h_m\}_{m \in \mathbb{Z}}$ be a frame and let $\{h^m\}_{m \in \mathbb{Z}}$ denote the dual frame. Then the set $\{\hat{h}_m\}_{m \in \mathbb{Z}}$ also constitutes a frame and the dual frame is defined by $(\hat{h})^m = 1/(2\pi)\widehat{h^m}$.

Proof. First of all, we show that the set $\{\hat{h}_m\}_{m \in \mathbb{Z}}$ with

$$\hat{h}_m(\omega) = \int_{\mathbb{R}} h_m(x) e^{-i\omega x} dx \quad (2.5)$$

is a frame. By Plancherel's theorem, we obtain

$$\begin{aligned}
A \|f\|_{L_2(\mathbb{R})}^2 &= 2\pi A \|\hat{f}\|_{L_2(\mathbb{R})}^2 \leq 2\pi \sum_{m \in \mathbb{Z}} |\langle \hat{f}, h_m \rangle|^2 \\
&= \sum_{m \in \mathbb{Z}} |\langle f, \hat{h}_m \rangle|^2 \leq 2\pi B \|\hat{f}\|_{L_2(\mathbb{R})}^2 = B \|f\|_{L_2(\mathbb{R})}^2.
\end{aligned} \tag{2.6}$$

It remains to identify the dual frame. The decomposition

$$f = \sum_{m \in \mathbb{Z}} \langle h_m, f \rangle h^m$$

implies

$$\hat{f} = \sum_{m \in \mathbb{Z}} \langle h_m, f \rangle \widehat{h^m} = \frac{1}{2\pi} \sum_{m \in \mathbb{Z}} \langle \hat{h}_m, \hat{f} \rangle \widehat{h^m},$$

and the result follows from another application of Plancherel's theorem. \square

Using the frame theoretic approach, the following reconstruction formula holds.

Theorem 2.2. Let $\{h_m\}_{m \in \mathbb{Z}}$ be a frame of outgoing signals in $L_2(\mathbb{R})$ and f_m denote the corresponding echoes produced by a reflectivity density $D(\tau, s)$,

$$f_m(t) = \int_{\mathbb{R}} \int_{\mathbb{R} \setminus \{0\}} D(\tau, s) |s|^{-1/2} h_m\left(\frac{t-\tau}{s}\right) \frac{ds d\tau}{s^2}. \tag{2.7}$$

Let us assume that the following conditions are satisfied:

$$\begin{aligned}
D(\tau, s) |s|^{-1/2} h_m\left(\frac{t-\tau}{s}\right) &\in L_1\left(\frac{ds dt d\tau}{s^2}\right), \\
\widehat{D(\cdot, s)}(\omega) &\in L_1(d\omega), \quad \widehat{D(\cdot, \sigma)}(\omega) |\sigma|^{-3/2} \in L_2(d\sigma).
\end{aligned} \tag{2.8}$$

Then $D(\tau, s)$ can be reconstructed as follows

$$\begin{aligned}
D(\tau, s) &= \frac{1}{(2\pi)^2} \sum_{m \in \mathbb{Z}} \int_{-\infty}^0 -\frac{1}{i} \widehat{f'_m}(\omega) \widehat{h^m}\left(\frac{\cdot}{s}\right)(\omega) |s|^{1/2} e^{i\tau\omega} d\omega \\
&\quad + \frac{1}{(2\pi)^2} \sum_{m \in \mathbb{Z}} \int_0^{\infty} \frac{1}{i} \widehat{f'_m}(\omega) \widehat{h^m}\left(\frac{\cdot}{s}\right)(\omega) |s|^{1/2} e^{i\tau\omega} d\omega,
\end{aligned} \tag{2.9}$$

where $\{h^m\}_{m \in \mathbb{Z}}$ denotes the dual frame of $\{h_m\}_{m \in \mathbb{Z}}$.

Proof. We first observe that

$$|s|^{-1/2} h_m\left(\frac{\cdot - \tau}{s}\right)(\omega) = |s|^{1/2} e^{-i\omega\tau} \hat{h}_m(\omega s). \tag{2.10}$$

Therefore, applying Fourier transforms to (2.7) and interchanging the order of integration, we get

$$\begin{aligned}
\hat{f}_m(\omega) &= \int_{\mathbb{R}} \int_{\mathbb{R} \setminus \{0\}} D(\tau, s) \int_{\mathbb{R}} |s|^{-1/2} h_m\left(\frac{t-\tau}{s}\right) e^{-i\omega t} dt \frac{ds d\tau}{s^2} \\
&= \int_{\mathbb{R}} \int_{\mathbb{R} \setminus \{0\}} D(\tau, s) |s|^{1/2} e^{-i\omega\tau} \hat{h}_m(s\omega) \frac{ds d\tau}{s^2} \\
&= \int_{\mathbb{R} \setminus \{0\}} \widehat{D(\cdot, s)}(\omega) \hat{h}_m(s\omega) |s|^{-3/2} ds.
\end{aligned}$$

Note that all modifications performed above are justified by (2.8). Hence, by employing the substitution $\sigma = s\omega$, we obtain

$$\begin{aligned}
\hat{f}_m(\omega) &= \int_{\mathbb{R} \setminus \{0\}} D\left(\cdot, \frac{\sigma}{\omega}\right)(\omega) \hat{h}_m(\sigma) \left|\frac{\sigma}{\omega}\right|^{-3/2} |\omega|^{-1} d\sigma \\
&= \int_{\mathbb{R} \setminus \{0\}} \tilde{D}(\omega, \sigma) \hat{h}_m(\sigma) d\sigma = \langle \tilde{D}(\omega, \cdot), \hat{h}_m(\cdot) \rangle,
\end{aligned} \tag{2.11}$$

where $\tilde{D}(\omega, \sigma)$ is defined by

$$\tilde{D}(\omega, \sigma) := D\left(\cdot, \frac{\sigma}{\omega}\right)(\omega) |\omega|^{1/2} |\sigma|^{-3/2}. \tag{2.12}$$

From (2.11), we see that the quantities $\hat{f}_m(\omega)$ can be interpreted as the coefficients of $\tilde{D}(\omega, \cdot)$ with respect to the set $\{\hat{h}_m\}_{m \in \mathbb{Z}}$. However, from lemma 2.1 we know that this set also constitutes a frame with a reciprocal frame $(\hat{h})^m = 1/(2\pi)\widehat{h^m}$. Therefore, by using the identity

$$f = \frac{1}{2\pi} \sum_{m \in \mathbb{Z}} \langle f, \hat{h}_m \rangle \widehat{h^m}, \tag{2.13}$$

we may reconstruct $\tilde{D}(\omega, \sigma)$ as

$$\tilde{D}(\omega, \sigma) = \frac{1}{2\pi} \sum_{m \in \mathbb{Z}} \langle \tilde{D}(\omega, \cdot), \hat{h}_m(\cdot) \rangle \widehat{h^m}(\sigma) = \frac{1}{2\pi} \sum_{m \in \mathbb{Z}} \hat{f}_m(\omega) \widehat{h^m}(\sigma). \tag{2.14}$$

From (2.14), we can now also reconstruct the density $D(\tau, s)$. By using definition (2.12), we obtain

$$D\left(\cdot, \frac{\sigma}{\omega}\right)(\omega) = \frac{1}{2\pi} \sum_{m \in \mathbb{Z}} \hat{f}_m(\omega) \widehat{h^m}(\sigma) |\sigma|^{3/2} |\omega|^{-1/2}$$

which yields

$$\begin{aligned}
\widehat{D(\cdot, s)}(\omega) &= \frac{1}{2\pi} \sum_{m \in \mathbb{Z}} \hat{f}_m(\omega) \widehat{h^m}(\omega s) |\omega| |s|^{3/2} \\
&= \frac{1}{2\pi} \sum_{m \in \mathbb{Z}} \hat{f}_m(\omega) |\omega| \widehat{h^m}\left(\frac{\cdot}{s}\right)(\omega) |s|^{1/2}.
\end{aligned} \tag{2.15}$$

Now the result follows applying the one-dimensional inverse Fourier transform to both sides of (2.15)

$$\begin{aligned}
D(\tau, s) &= \frac{1}{2\pi} \int_{\mathbb{R}} \widehat{D(\cdot, s)}(\omega) e^{i\tau\omega} d\omega \\
&= \frac{1}{(2\pi)^2} \sum_{m \in \mathbb{Z}} \int_{\mathbb{R}} \hat{f}_m(\omega) |\omega| h^m\left(\frac{\cdot}{s}\right)(\omega) |s|^{1/2} e^{i\tau\omega} d\omega \\
&= \frac{1}{(2\pi)^2} \sum_{m \in \mathbb{Z}} \int_{-\infty}^0 -\omega \hat{f}_m(\omega) h^m\left(\frac{\cdot}{s}\right)(\omega) |s|^{1/2} e^{i\tau\omega} d\omega \\
&\quad + \frac{1}{(2\pi)^2} \sum_{m \in \mathbb{Z}} \int_0^{\infty} \omega \hat{f}_m(\omega) h^m\left(\frac{\cdot}{s}\right)(\omega) |s|^{1/2} e^{i\tau\omega} d\omega \\
&= \frac{1}{(2\pi)^2} \sum_{m \in \mathbb{Z}} \int_{-\infty}^0 -\frac{1}{i} \hat{f}'_m(\omega) h^m\left(\frac{\cdot}{s}\right)(\omega) |s|^{1/2} e^{i\tau\omega} d\omega \\
&\quad + \frac{1}{(2\pi)^2} \sum_{m \in \mathbb{Z}} \int_0^{\infty} \frac{1}{i} \hat{f}'_m(\omega) h^m\left(\frac{\cdot}{s}\right)(\omega) |s|^{1/2} e^{i\tau\omega} d\omega. \quad \square
\end{aligned}$$

We would like to conclude this section on reconstruction formulae for wideband radar models with a reference to an elegant but rather different approach. Assume that the signal $h_m(t) \sim \delta(t - t_m)$ is a short pulse at time t_m . Then, the echo (1.4) at time t is equivalent to the integration of D along the line $\tau = t - st_m$. I.e., if echoes resemble the Radon transform of D , then they can be inverted by tomographic inversion procedures, see [6].

3. Error estimates

In the previous section, we have derived a method to reconstruct the reflectivity density from the observed echoes. However, the applicability of this method to real-life problems is diminished by the fact that the underlying frame usually contains *infinitely* many elements. Clearly, in practice, only a finite number of frame elements can be transmitted. Hence we face the problem of choosing appropriate collections. Furthermore, it is clearly desirable to have some information concerning the resulting approximation properties for different choices of frames.

The derivation of the error bounds rests on a Jackson type estimate for the frame $\{\widehat{h}^m\}_{m \in \mathbb{Z}}$. Let us assume that this set of functions allows an ordering by index sets $I_J \subset \mathbb{Z}$, such that a Jackson-type estimate of the form

$$\left\| g - \frac{1}{2\pi} \sum_{m \in I_J} \langle g, \hat{h}_m \rangle \widehat{h}^m \right\|_{L_2(\mathbb{R})}^2 \lesssim 2^{-2J\alpha} |g|_{H^\alpha(\mathbb{R})}^2 \quad (3.1)$$

holds. (In the sequel, \lesssim will always indicate inequality up to constant factors.) H^α denotes the Sobolev space of order α , see, e.g., [1].

Such estimates are known for a variety of functions, e.g., trigonometric polynomials and hierarchical finite elements. In the context of wavelet analysis, this requirement is met by orthogonal or biorthogonal wavelets. If (3.1) is valid, the following result in the weighted L_2 -space $L_2(\mathbb{R}^2, d\tau ds/|s|^3)$ holds.

Theorem 3.1. Suppose that for some fixed α a Jackson-type estimate of the form (3.1) holds and that the condition

$$G(\alpha, \omega) := |\tilde{D}(\omega, \cdot)|_{H^\alpha(\mathbb{R})}^2 < \infty \quad (3.2)$$

is satisfied. Then, the following error estimate is valid:

$$\begin{aligned} & \int_{\mathbb{R}} \int_{\mathbb{R}} \left| D(\tau, s) - \frac{1}{(2\pi)^2} \sum_{m \in I_J} \int_{\mathbb{R}} \hat{f}_m(\omega) \hat{h}_m(s\omega) |\omega| |s|^{3/2} e^{i\tau\omega} d\omega \right|^2 d\tau \frac{ds}{|s|^3} \\ & \lesssim 2^{-2J\alpha} \int_{\mathbb{R}} |\omega| G(\alpha, \omega) d\omega. \end{aligned} \quad (3.3)$$

If α is an integer, the function $G(\alpha, \omega)$ can be estimated in terms of the density D as follows:

$$G(\alpha, \omega) \lesssim \sum_{\beta \leq \alpha} |\omega|^{1+2\beta-2\alpha} \int_{\mathbb{R}} \left| \widehat{\left(\frac{\partial^{\alpha-\beta}}{\partial \sigma} D \right)} \left(\cdot, \frac{\sigma}{\omega} \right) (\omega) \sigma^{3/2-\beta} \right|^2 d\sigma. \quad (3.4)$$

Proof. In our setting, the Jackson-type estimate (3.1) applied to $g = \tilde{D}(\omega, \cdot)$ reads as follows:

$$\left\| \tilde{D}(\omega, \cdot) - \frac{1}{(2\pi)} \sum_{m \in I_J} \hat{f}_m(\omega) \hat{h}_m(\cdot) \right\|_{L_2(\mathbb{R})}^2 \lesssim 2^{-2J\alpha} |\tilde{D}(\omega, \cdot)|_{H^\alpha(\mathbb{R})}^2. \quad (3.5)$$

Hence, by using (2.12) and substituting $\sigma = s\omega$ we obtain

$$\begin{aligned} 2^{-2J\alpha} G(\alpha, \omega) & \gtrsim \left\| D \left(\cdot, \frac{\sigma}{\omega} \right) (\omega) |\omega|^{1/2} |\sigma|^{-3/2} - \frac{1}{2\pi} \sum_{m \in I_J} \hat{f}_m(\omega) \hat{h}_m(\sigma) \right\|_{L_2(d\sigma)} \\ & = \int_{\mathbb{R}} \left| \widehat{D}(\cdot, s)(\omega) - \frac{1}{2\pi} \sum_{m \in I_J} \hat{f}_m(\omega) \hat{h}_m(s\omega) |\omega| |s|^{3/2} \right|^2 |\omega| |\omega|^{-2} \frac{ds}{|s|^3}. \end{aligned} \quad (3.6)$$

Therefore, multiplying both sides of (3.6) by $|\omega|$, integrating with respect to ω , and applying Plancherel's theorem to another time, we have

$$\begin{aligned}
& 2^{-2J\alpha} \int_{\mathbb{R}} |\omega| G(\alpha, \omega) \, d\omega \\
& \gtrsim \int_{\mathbb{R}} \int_{\mathbb{R}} \left| \widehat{D(\cdot, s)}(\omega) - \frac{1}{2\pi} \sum_{m \in I_J} \hat{f}_m(\omega) \hat{h}_m(s\omega) |\omega| |s|^{3/2} \right|^2 \frac{d\omega \, ds}{|s|^3} \\
& = 2\pi \int_{\mathbb{R}} \int_{\mathbb{R}} \left| D(\tau, s) - \frac{1}{(2\pi)^2} \sum_{m \in I_J} \int_{\mathbb{R}} \hat{f}_m(\omega) \hat{h}_m(s\omega) |\omega| |s|^{3/2} e^{i\tau\omega} \, d\omega \right|^2 \frac{d\tau \, ds}{|s|^3}.
\end{aligned} \tag{3.7}$$

It remains to establish (3.4). By using Leibniz' rule, we obtain

$$\begin{aligned}
|\tilde{D}(\omega, \cdot)|_{H^\alpha(\mathbb{R})}^2 &= \int_{\mathbb{R}} \left| \frac{\partial^\alpha}{\partial \sigma} (\tilde{D}(\omega, \cdot)) \right|^2 \, d\sigma \\
&= \int_{\mathbb{R}} \left| \frac{\partial^\alpha}{\partial \sigma} \left(D\left(\cdot, \frac{\sigma}{\omega}\right) |\omega|^{1/2} |\sigma|^{-3/2} \right) \right|^2 \, d\sigma \\
&= |\omega| \int_{\mathbb{R}} \left| \frac{\partial^\alpha}{\partial \sigma} \left(\int_{\mathbb{R}} D\left(\tau, \frac{\sigma}{\omega}\right) e^{i\omega\tau} \, d\tau \sigma^{-3/2} \right) \right|^2 \, d\sigma \\
&= |\omega| \int_{\mathbb{R}} \left| \sum_{\beta \leq \alpha} \binom{\alpha}{\beta} \frac{\partial^{\alpha-\beta}}{\partial \sigma} \left(\int_{\mathbb{R}} D\left(\tau, \frac{\sigma}{\omega}\right) e^{-i\omega\tau} \, d\tau \right) \left(\frac{\partial^\beta}{\partial \sigma} \sigma^{-3/2} \right) \right|^2 \, d\sigma \\
&= |\omega| \int_{\mathbb{R}} \left| \sum_{\beta \leq \alpha} \binom{\alpha}{\beta} \left(\int_{\mathbb{R}} \left(\frac{\partial^{\alpha-\beta}}{\partial \sigma} D \right) \left(\tau, \frac{\sigma}{\omega} \right) \omega^{\beta-\alpha} e^{-i\omega\tau} \, d\tau \right) \right. \\
&\quad \times \left. \left(-\frac{3}{2} \right) \left(-\frac{3}{2} - 1 \right) \cdots \left(-\frac{3}{2} - \beta - 1 \right) \sigma^{-3/2-\beta} \right|^2 \, d\sigma \\
&= |\omega| \int_{\mathbb{R}} \left| \sum_{\beta \leq \alpha} \binom{\alpha}{\beta} \left(\frac{\partial^{\alpha-\beta}}{\partial \sigma} D \right) \left(\cdot, \frac{\sigma}{\omega} \right) (\omega) \right. \\
&\quad \times \left. \omega^{\beta-\alpha} \prod_{l=0}^{\beta-1} \left(-\frac{3}{2} - l \right) \sigma^{-3/2-\beta} \right|^2 \, d\sigma \\
&\lesssim \sum_{\beta \leq \alpha} |\omega|^{1+2\beta-2\alpha} \int_{\mathbb{R}} \left| \left(\frac{\partial^{\alpha-\beta}}{\partial \sigma} D \right) \left(\cdot, \frac{\sigma}{\omega} \right) (\omega) \sigma^{-3/2-\beta} \right|^2 \, d\sigma,
\end{aligned}$$

and (3.4) is shown. \square

Now, let us consider a special case that the frames $\{h_m\}_{m \in \mathbb{Z}}$ and $\{h^m\}_{m \in \mathbb{Z}}$ consist of the inverse Fourier transforms of the elements of a biorthogonal wavelet basis, i.e.,

$$\begin{aligned}
h_m &= h_{m(j,k)} = \mathcal{F}^{-1} \psi_{j,k}, & h^m &= h^{m(j,k)} = 2\pi \mathcal{F}^{-1} \tilde{\psi}_{j,k}, \\
\psi_{j,k}(x) &= 2^{j/2} \psi(2^j x - k), & j, k &\in \mathbb{Z},
\end{aligned} \tag{3.8}$$

where the functions $\psi_{j,k}$ and $\tilde{\psi}_{j,k}$ satisfy

$$\langle \psi_{j,k}, \tilde{\psi}_{j',k'} \rangle = \delta_{j,j'} \delta_{k,k'}. \quad (3.9)$$

We may, e.g., use the compactly supported wavelet basis constructed by Daubechies [3] or the biorthogonal wavelet basis developed by Cohen et al. [2]. Then we do not employ all functions in the resulting frame, but only those up to a given refinement level J . The resulting error estimate reads as follows.

Corollary 3.1. Let $N - 1$ denote the degree of polynomial exactness of the multiresolution analysis $\{\tilde{V}_j\}_{j \in \mathbb{Z}}$ associated with the dual wavelet $\tilde{\psi}$. Suppose that, for some fixed $\alpha < N$, condition (3.2) holds. Then, the following error estimate is valid:

$$\begin{aligned} & \int_{\mathbb{R}} \int_{\mathbb{R}} \left| D(\tau, s) - \frac{1}{(2\pi)^2} \sum_{j \leq J} \int_{\mathbb{R}} \hat{f}_m(\omega) \hat{h}_m(s\omega) |\omega| |s|^{3/2} e^{i\tau\omega} d\omega \right|^2 d\tau \frac{ds}{|s|^3} \\ & \lesssim 2^{-2J\alpha} \int_{\mathbb{R}} |\omega| G(\alpha, \omega) d\omega. \end{aligned} \quad (3.10)$$

Proof. The classical wavelet analysis provides us with the Jackson-type estimate

$$\left\| g - \sum_{k \in \mathbb{Z}, j \leq J} \langle g, \psi_{j,k} \rangle \tilde{\psi}_{j,k} \right\|_{L_2(\mathbb{R})}^2 \lesssim 2^{-2\alpha J} |g|_{H^\alpha(\mathbb{R})}^2, \quad (3.11)$$

see, e.g., [4] for details. Now the result follows from theorem 3.1. \square

Remark 3.1. The polynomial exactness is closely related with the regularity of the wavelet basis, see [3] for details.

4. The multivariate case

In this section, we want to investigate to what extent the analysis presented above can be generalized to the multivariate case. In the sequel, we shall focus especially on the 2D-case. First of all, we have to derive a suitable mathematical model which describes the echoes produced by a 2-dimensional reflectivity distribution. Secondly, we have to analyze how this reflectivity density can be reconstructed from these echoes.

4.1. A 2D-model

For univariate signals in $L_2(\mathbb{R})$, model (1.4) which describes the echoes produced by a reflectivity density is well-established. This model deals with signals which are modulated over time, i.e., the signal is a function $h(t)$. However, this allows us only to reconstruct the velocities in the direction of the emitted beam, i.e., only the radial component of the velocity field can be analyzed.

It seems that much less is known in higher-dimensional cases. In general, one might assume that the signal is emitted in a three-dimensional cone. In principle, one might then emit signals, which are modulated differently for each beam in this cone, i.e., the emitted signal is a function $h(t, \gamma, \zeta)$, where γ and ζ are angles of the cone.

In this paper, we want to treat a two-dimensional model as a first step. We assume here that the signal is emitted as a fan. Moreover, we assume that the positions of the reflecting entities, as described by the support of the reflectivity distribution D , are sufficiently far away, so that we can treat the fan of beams as a set of parallel beams instead. Let us assume that the beams are aligned on the x -axis, i.e., the emitted signal is modelled by a function $h(t, x)$, and that the signal is emitted in the direction of the y -axis.

We follow the approach of section 1 in order to model the resulting echoes mathematically. Hence, let us first consider the case of a single-point object, which is moving in the (x, y) -plane. We further assume that the measurement process lasts for a shorter time scale as compared to the velocity of the object. Hence, we can neglect any acceleration of the object and simply assume that the trajectory of the object is given by

$$(x(t), y(t)) = (x_0 + tv_x, y_0 + tv_y). \quad (4.1)$$

Again, we introduce Doppler variables

$$s_0 := \frac{c + v_y}{c - v_y}, \quad \tau_0 := \frac{2y_0}{c - v_y}. \quad (4.2)$$

At time t the moving object is in a position with the y -coordinate $y_0 + tv_y$, i.e., at this instant it reflects a signal which was send out at time $t - (y_0 + tv_y)/c$ in the corresponding position $x_0 + tv_x$. Altogether, the object reflects the signal

$$s(t) = h\left(t - \frac{y_0 + tv_y}{c}, x_0 + tv_x\right).$$

This signal then produces an echo in the position $x = x_0 + tv_x$ which is time delayed by $(y_0 + tv_y)/c$, i.e., this yields an echo

$$e\left(t + \frac{y_0 + tv_y}{c}, x_0 + tv_x\right) = s(t) = h\left(t - \frac{y_0 + tv_y}{c}, x_0 + tv_x\right). \quad (4.3)$$

We define the auxiliary parameters

$$\sigma_0 := v_x \frac{1 + s_0}{2s_0} \quad \text{and} \quad z_0 = x_0 - \frac{v_x \tau_0}{2s_0}. \quad (4.4)$$

Lemma 4.1. Suppose that the object is moving at the velocity $v = (v_x, v_y)$ in the (x, y) -plane and that a signal $h(x, t)$ is transmitted. Then the echo produced by the object is given by

$$e(t, z_0 + t\sigma_0) = h\left(\frac{t - \tau_0}{s_0}, z_0 + t\sigma_0\right). \quad (4.5)$$

Proof. We start from equation (4.3) and use the substitution $t \rightarrow t + (y_0 + tv_y)/c$, which yields

$$e\left(t, x_0 + \left(\frac{ct - y_0}{c + v_y}\right)v_x\right) = h\left(\left(\frac{ct - y_0}{c + v_y}\right)\frac{c - v_y}{c} - \frac{y_0}{c}, x_0 + \left(\frac{ct - y_0}{c + v_y}\right)v_x\right).$$

Rewriting this equation in Doppler coordinates and using the auxiliary parameters (4.4) we get

$$e\left(t, z_0 + t\sigma_0\right) = h\left(\frac{t - \tau_0}{s_0}, z_0 + t\sigma_0\right). \quad (4.6)$$

and the lemma is proved. \square

The set of parameters $(\tau_0, s_0, z_0, \sigma_0)$ is in one-to-one correspondence to the original variables (x_0, v_x, y_0, v_y) . Hence, similarly to the 1D-case, we describe a dense target environment by a reflectivity distribution $D(\tau_0, s_0, z_0, \sigma_0)$. Note that we use slightly different notation for the Doppler coordinates in the 2D-case: the variable s in the 1D-model corresponds to the variable $1/s_0$ in the 2D-case. This avoids the term ds/s^2 , moreover, we have neglected the scaling term \sqrt{s} . We now obtain the following model for describing the 2D-echo.

Corollary 4.1. The echo produced by a reflectivity density $D(\tau_0, s_0, z_0, \sigma_0)$ is given by

$$e(t, x) = \int_{\mathbb{R}} \int_{\mathbb{R}} \int_{\mathbb{R}} \int_{\mathbb{R}} D(\tau_0, s_0, z_0, \sigma_0) \delta(x - (z_0 + \sigma_0 t)) \times h\left(\frac{t - \tau_0}{s_0}, z_0 + \sigma_0 t\right) d\tau_0 ds_0 d\sigma_0 dz_0. \quad (4.7)$$

Proof. We rewrite the echo of a single object as

$$e(t, x) := \delta(x - (z_0 + \sigma_0 t)) h\left(\frac{t - \tau_0}{s_0}, z_0 + \sigma_0 t\right). \quad (4.8)$$

Consequently, for the case of a nontrivial reflectivity density, we obtain

$$e(t, x) = \int_{\mathbb{R}} \int_{\mathbb{R}} \int_{\mathbb{R}} \int_{\mathbb{R}} D(\tau_0, s_0, z_0, \sigma_0) \delta(x - (z_0 + \sigma_0 t)) \times h\left(\frac{t - \tau_0}{s_0}, z_0 + \sigma_0 t\right) d\tau_0 ds_0 d\sigma_0 dz_0,$$

proving the corollary. \square

4.2. The reconstruction problem

Once the model described in corollary 4.1 is given, it is natural to ask for a suitable reconstruction formula to extract the unknown density D . Again we suggest transmitting

not just one signal, but a family of signals. However, even then, in contrast to the univariate case, the density cannot be completely reconstructed. The operator which maps the reflectivity density to its echoes is linear, hence it makes sense to characterize the null-space of this mapping.

Definition 4.1. A function $D \in L_2(\mathbb{R}^4)$ is called a vanishing reflectivity distribution if the echo (4.7) vanishes for any signal $h \in L_2(\mathbb{R}^2)$.

These vanishing reflectivity distributions can be characterized by their integrals over certain 2D-subspaces. Let $E(\tau, x, \nu)$ denote a 2D-plane defined by

$$E(t, x, \nu) = \{(\tau_0, s_0, z_0, \sigma_0) \mid \tau_0 = t - \nu s_0, z_0 = x - \sigma_0 t, s_0, \sigma_0 \in \mathbb{R}\}.$$

The null-space is then characterized by the following lemma.

Lemma 4.2. A function $D \in L_2(\mathbb{R}^4)$ is a vanishing reflectivity distribution if and only if the integrals of $s_0 D$ over the 2D-planes

$$\{E(t, x, \nu) \mid t, x, \nu \in \mathbb{R}\}$$

vanish, i.e.,

$$0 = \int_{\mathbb{R}} \int_{\mathbb{R}} s_0 D(t - \nu s_0, s_0, x - \sigma_0 t, \sigma_0) ds_0 d\sigma_0,$$

for all $(t, x, \nu) \in \mathbb{R}^3$.

Proof. In order to show that the echoes of reflectivity distribution vanish for all signals $h \in L_2(\mathbb{R}^2)$, it suffices that the echoes vanish for all separable signals

$$h(t, x) = h_1(t)h_2(x).$$

Inserting this into the model of the echo (4.7) and applying the substitution $\nu = (t - \tau_0)/s_0$, we obtain

$$\begin{aligned} e(t, x) &= \int_{\mathbb{R}} \int_{\mathbb{R}} \int_{\mathbb{R}} \int_{\mathbb{R}} D(\tau_0, s_0, z_0, \sigma_0) \delta(x - (z_0 + \sigma_0 t)) \\ &\quad \times h_1\left(\frac{t - \tau_0}{s_0}\right) h_2(z_0 + \sigma_0 t) d\tau_0 ds_0 d\sigma_0 dz_0 \\ &= h_2(x) \int_{\mathbb{R}} \int_{\mathbb{R}} \int_{\mathbb{R}} D(\tau_0, s_0, x - \sigma_0 t, \sigma_0) h_1\left(\frac{t - \tau_0}{s_0}\right) d\tau_0 ds_0 d\sigma_0 \\ &= h_2(x) \int_{\mathbb{R}} \int_{\mathbb{R}} \int_{\mathbb{R}} s_0 D(t - \nu s_0, s_0, x - \sigma_0 t, \sigma_0) h_1(\nu) d\nu ds_0 d\sigma_0. \end{aligned}$$

These integrals have to vanish for any choice of t and x . Moreover, with respect to the variable v , the scalar products with all $h_1 \in L_2(\mathbb{R})$ have to vanish, i.e., a vanishing reflectivity distribution has to satisfy a.e.

$$0 = \int_{\mathbb{R}} \int_{\mathbb{R}} s_0 D(t - v s_0, s_0, x - \sigma_0 t, \sigma_0) \, ds_0 \, d\sigma_0,$$

which yields the desired characterization of the null-space by vanishing integrals of D over 2D-planes. \square

Vanishing integrals can only occur if the integrand takes positive and negative values. However, a physically meaningful reflectivity distribution is non-negative, and s_0 lives on the positive part of the real line. Nevertheless, two positive reflectivity distributions D_1 and D_2 which only differ by a vanishing reflectivity distribution, cannot be distinguished by any combination of transmitted signals.

The null-space is characterized by a three-dimensional set of conditions. In order to characterize the complement of the null-space, i.e., the reconstructable reflectivity distributions, we need to eliminate one of the four variables of $D \in L_2(\mathbb{R}^4)$.

This can be achieved by reducing the dependency of D on σ_0 , by fixing the mean velocity as follows: we define

$$\mathcal{D}(\tau_0, s_0, x, t) := \int_{\mathbb{R}} D(\tau_0, s_0, x - \sigma_0 t, \sigma_0) \, d\sigma_0 \quad (4.9)$$

and assume that \mathcal{D} can be approximated by its zero order term

$$\mathcal{D}(\tau_0, s_0, x, t) \sim \mathcal{D}\left(\tau_0, s_0, x, \frac{v_0}{c}\right). \quad (4.10)$$

Furthermore, we have to assume that the family of transmitted signals consists of tensor products

$$h_{m,n}(x, t) := h_m(t)h_n(x), \quad (4.11)$$

where both families $\{h_m\}_{m \in \mathbb{Z}}$ and $\{h_n\}_{n \in \mathbb{Z}}$ form frames in $L_2(\mathbb{R})$.

The first step is to integrate (4.7) with respect to z_0 , and this yields

$$\begin{aligned} e(\tau, x) &= \int_{\mathbb{R}} \int_{\mathbb{R}} \int_{\mathbb{R}} D(\tau_0, s_0, x - \sigma_0 t, \sigma_0) h_{m,n}\left(\frac{\tau - \tau_0}{s_0}, x\right) \, d\sigma_0 \, d\tau_0 \, ds_0 \\ &= \int_{\mathbb{R}} \int_{\mathbb{R}} \mathcal{D}(\tau_0, s_0, x, t) h_m\left(\frac{\tau - \tau_0}{s_0}\right) h_n(x) \, d\tau_0 \, ds_0 \\ &\sim h_n(x) \int_{\mathbb{R}} \int_{\mathbb{R}} \mathcal{D}\left(\tau_0, s_0, x, \frac{v_0}{c}\right) h_m\left(\frac{\tau - \tau_0}{s_0}\right) \, d\tau_0 \, ds_0. \end{aligned} \quad (4.12)$$

Now the quantity $\mathcal{D}(\tau_0, s_0, x, v_0/c)$ can be reconstructed, by using the method explained in section 2.

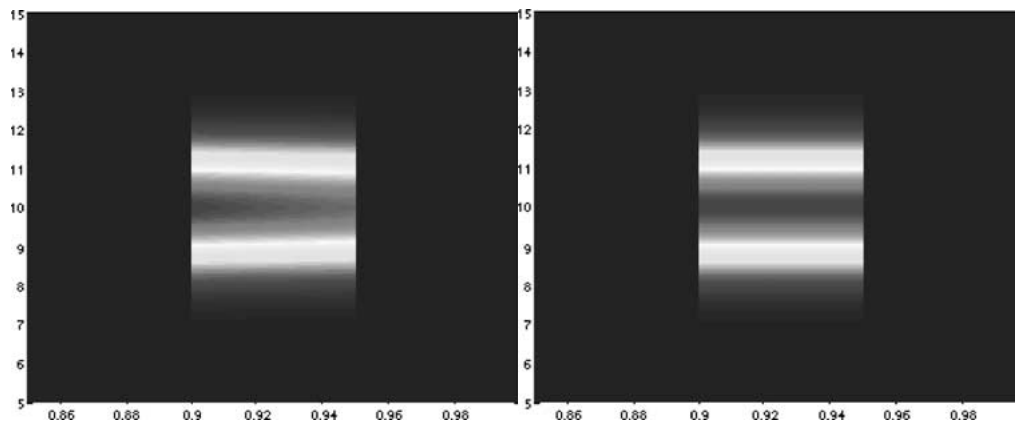


Figure 1. Representation of $\widehat{D(\cdot, s)}(\omega)$ and $\widehat{D(\cdot, s)}(\omega)|s|^{-3/2}$ on the discrete grid $[5.00, 15.00] \times [0.85, 1.00]$.

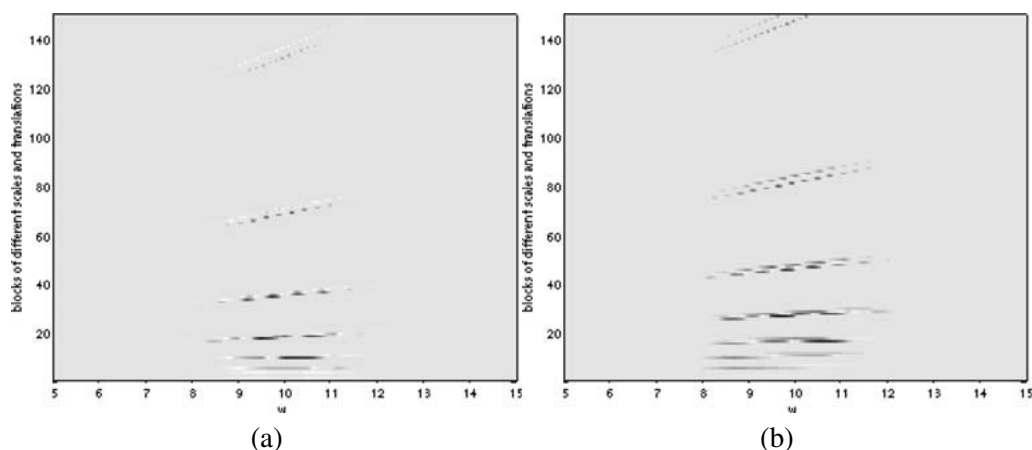


Figure 2. The simulated echoes $\{\hat{f}_m\}_{m \in \mathbb{Z}}$ for the Haar frame (a) and the Daubechies-5-frame (b). The higher scales are not displayed.

5. Numerical experiments

In this section, we want to demonstrate the applicability of our reconstruction formulae and the error estimates presented above. The application of our theory to real-life data is still in its elaboration. In particular, 2D-data for signals, which can be modulated arbitrarily in time t and position x , are not available. Nevertheless, to test the algorithm, we proceed as follows: we fix in advance an (artificial) density D in range Doppler coordinates and a suitable frame $\{h_m\}_{m \in \mathbb{Z}}$, compute the corresponding echoes, and apply the reconstruction procedure to these echoes. The true density is known in this case, hence, we can estimate and compare the error bounds of different approximation schemes.

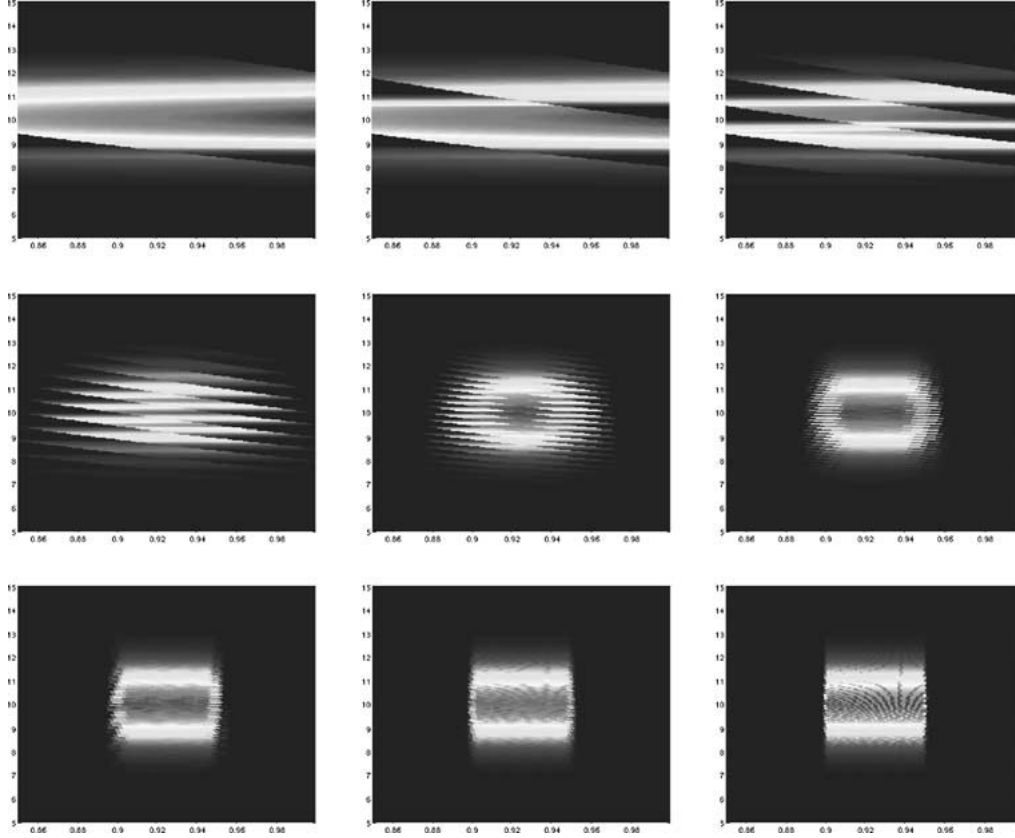


Figure 3. Partial reconstructions based on simulated echoes with respect to the Haar frame. The shown images correspond to the reconstructed densities for $J = -3, -2, -1, 0, 1, 2, 3, 4$ and 6 (from top left to bottom right).

First of all, we fix a density D which fits into the setting of our theory: as a manageable example we choose D as

$$D(\tau, s) := e^{i\tau\omega_0} e^{-\tau^2/2} \mathbb{1}_{[-s_1, s_2]}(s),$$

where $\mathbb{1}_{[-s_1, s_2]}$ represents the characteristic function of the closed interval $[-s_1, s_2]$ and ω_0 describes a shift in the Fourier domain. In the sequel, we choose $s_1 = 0.90$ and $s_2 = 0.95$. This reflectivity distribution D satisfies the assumptions of theorem 2.2.

The outgoing signals have to be a frame. However, since we also want to verify the error estimate in theorem 3.1. Corollary 3.1 indicates that a good choice for the frame is given by

$$h_m(t) = h_{m(j,k)}(t) := \mathcal{F}^{-1} \psi_{j,k}(t),$$

where $\mathcal{F}^{-1} \psi_{j,k}$ is the inverse Fourier transform of some dilated and translated wavelet, see formula (3.8). In our simulations we used the Haar basis, the Daubechies wavelets of order two (compare [3]), and biorthogonal wavelets as constructed in [2], respectively.

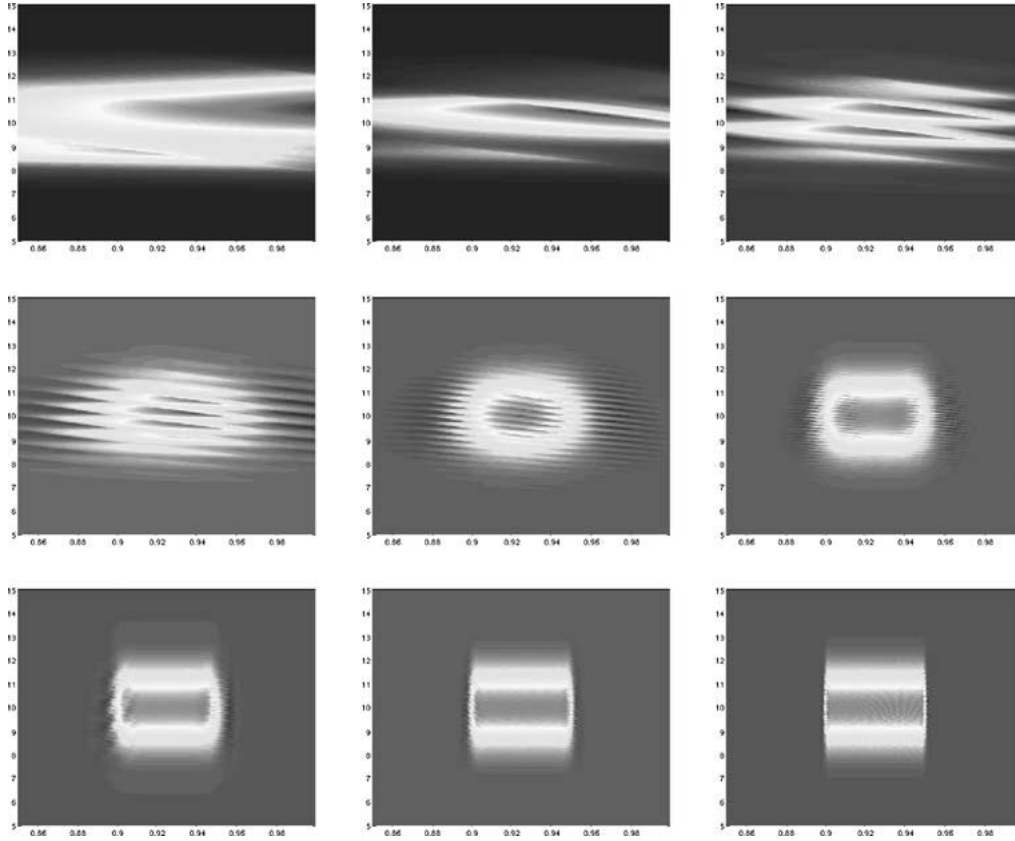


Figure 4. Partial reconstructions based on simulated echoes with respect to the Daubechies frame ($N = 2$). The shown images correspond to the reconstructed densities for $J = -3, -2, -1, 0, 1, 2, 3, 4$ and 6 (from top left to bottom right).

Basing on the underlying density D , we now have to generate families of echoes $\{f_m\}_{m \in \mathbb{Z}}$ which represent the backscattered signals of the transmitted frame $\{h_m\}_{m \in \mathbb{Z}}$. Using the substitution (2.12), we approximate the echoes

$$\hat{f}_m(\omega) = \int_{\mathbb{R} \setminus \{0\}} \widehat{D(\cdot, s)}(\omega) \hat{h}_m(s\omega) |s|^{-3/2} ds$$

by the corresponding Riemann sums for evaluating these L_2 -inner products. A rough approximation is then given by

$$\begin{aligned} \hat{f}_{j,k}(\omega) &\approx \sum_{s_l \in \Lambda_s} \widehat{D(\cdot, s_l)}(\omega) \psi_{j,k}(\omega s_l) |s_l|^{-3/2} h_l \\ &= \sum_{s_l \in \Lambda_s} e^{-(\omega - \omega_0)^2 / 2} \mathbb{1}_{[0.90, 0.95]}(s_l) 2^{j/2} \psi(2^j \omega s_l - k) |s_l|^{-3/2} h_l, \end{aligned} \quad (5.1)$$

where Λ_s describes the grid with respect to the variable s and $h_l = s_l - s_{l-1}$.

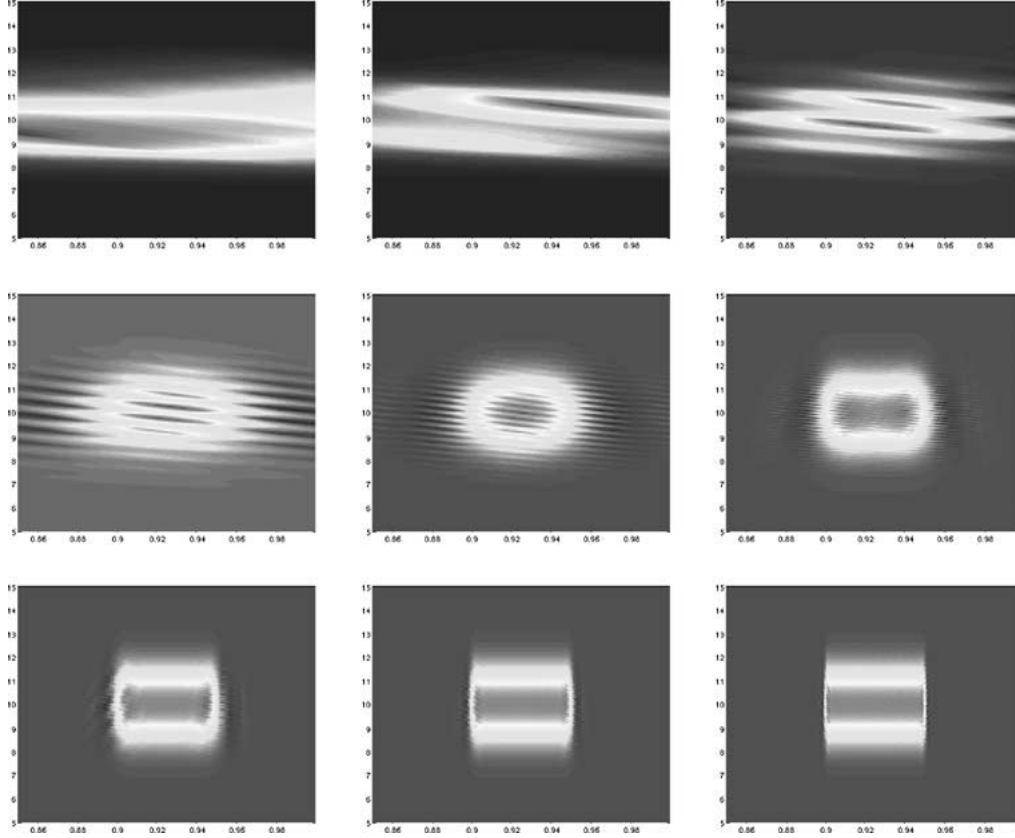


Figure 5. Partial reconstructions based on simulated echoes with respect to the Bior2.4 frame. The shown images correspond to the reconstructed densities for $J = -3, -2, -1, 0, 1, 2, 3, 4$ and 6 (from top left to bottom right).

Numerically we have to truncate the evaluation of the echoes at some index (j, k) . The numerical implementations start at the resolution level $j_{\min} = -3$ and end at $j_{\max} = 6$. On the first approximation level $j_{\min} = -3$, we use the echoes produced by translations of the corresponding generator function φ , see again [3] for further information.

For our discretization, we choose $s_l = 0.85 + h_l$, where $h_l = l \cdot 0.00035$ and $l = 0, \dots, 429$, and $w_r = 5.00 + v_r$, where $v_r = r \cdot 0.025$ and $r = 0, \dots, 399$. Hence, we have to choose the translation parameter k in such a way that – for all relevant j, r and l – the value of $2^j \omega_r s_l - k$ covers the support of ψ and φ . Figure 1 displays the functions $\widehat{D(\cdot, s)}(\omega)$ and $\widehat{D(\cdot, s)}(\omega)|s|^{-3/2}$ on the rectangle $[5.00, 15.00] \times [0.85, 1.00]$. The resulting echoes approximated by (5.1) are visualized in figure 2.

Now we are ready to apply the reconstruction formula stated in theorem 2.2. In order to keep the technical difficulties at a reasonable level, we restrict ourselves to the

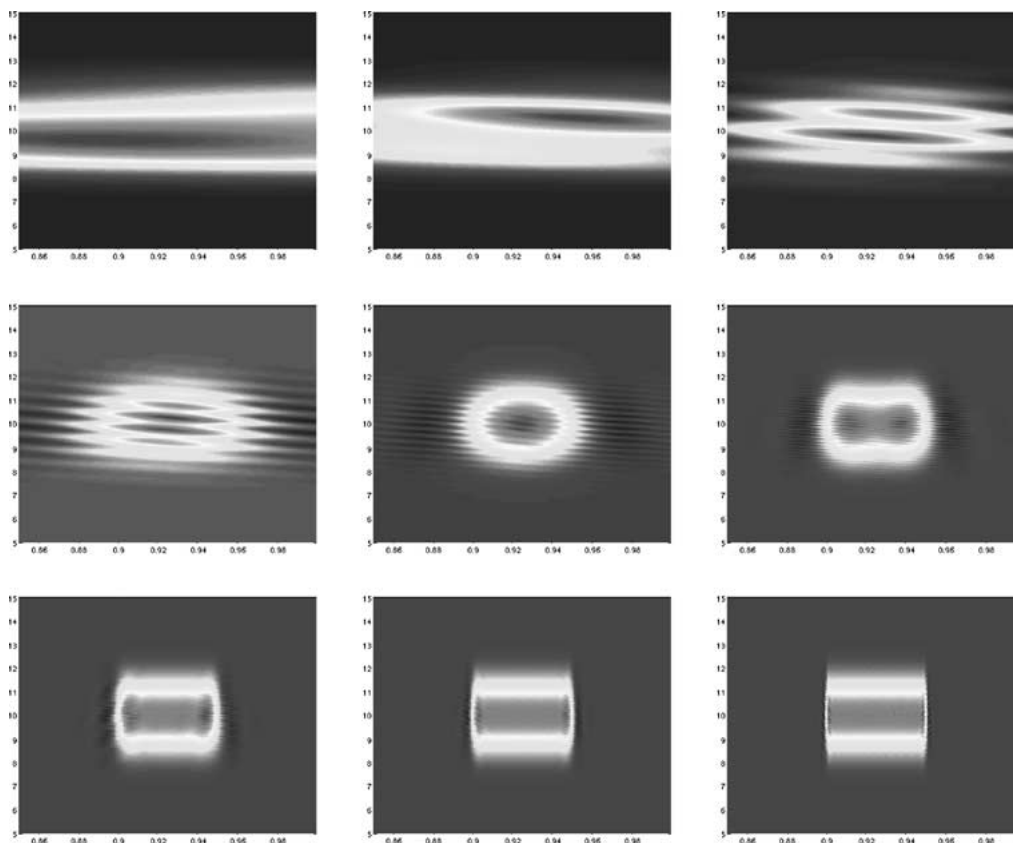


Figure 6. Partial reconstructions based on simulated echoes with respect to the Bior 2.8 frame. The shown images correspond to the reconstructed densities for $J = -3, -2, -1, 0, 1, 2, 3, 4$ and 6 (from top left to bottom right).

reconstruction in the Fourier domain:

$$\widehat{D(\cdot, s)}(\omega) = \frac{1}{2\pi} \sum_{m \in \mathbb{Z}} \hat{f}_m(\omega) \widehat{h^m}(\omega s) |\omega| |s|^{3/2}.$$

The quality of reconstruction is estimated by computing the left-hand side of the error estimate of corollary 3.1. The appraisal has to be taken modulo the integration and scale projection error. The error estimation in corollary 3.1 was stated in the time domain, Plancherel's theorem, however, translates this into an identical estimate in the Fourier domain representation, see (3.7). Additionally, corollary 3.1 predicts an exponential decay of the error rate, the constants of the estimate depend on the regularity of the frame. Indeed, we observe that the weighted L_2 -error decreases in the predicted way as the frame regularity increases: we start by presenting a scale-wise reconstruction, see figures 3–6. It turns out that the algorithm converges for all simulated cases. Following

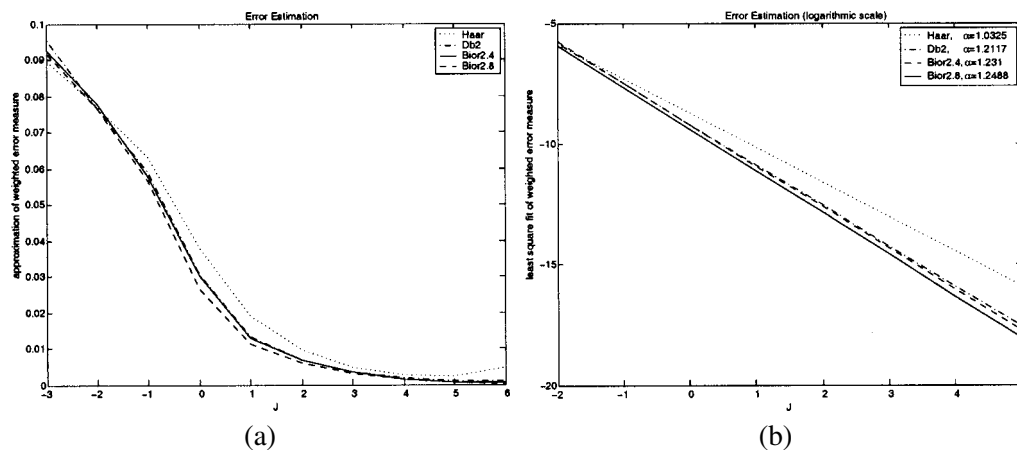


Figure 7. The weighted L_2 -error: (a) shows the numerically evaluated error, and (b) the linear least squares fit in the logarithmic scale.

corollary 3.1, we study the error depending on the scale J and on the frame regularity α , respectively. Therefore it is necessary to plot

$$\int_{\mathbb{R}} \int_{\mathbb{R}} \left| \widehat{D}(\cdot, s)(\omega) - \frac{1}{2\pi} \sum_{j \leq J} \hat{f}_m(\omega) \hat{h}_m(s\omega) |\omega| |s|^{3/2} \right|^2 d\omega \frac{ds}{|s|^3}.$$

From figure 7(a), we see that the error decreases exponentially indeed. From the logarithmic plot, figure 7(b), we can estimate the parameter α as the slope of the linear least squares fit. We deduce the validity of the proposed wavelet-based reconstruction algorithm and of the given error estimate.

References

- [1] R.A. Adams, *Sobolev Spaces* (Academic Press, New York, 1975).
- [2] A. Cohen, I. Daubechies and J. Feauveau, Biorthogonal bases of compactly supported wavelets, *Comm. Pure Appl. Math.* 45 (1992) 485–560.
- [3] I. Daubechies, *Ten Lectures on Wavelets*, CBMS–NSF Regional Conference Series in Applied Mathematics, Vol. 61 (SIAM, Philadelphia, PA, 1992).
- [4] R. DeVore, Nonlinear approximation, *Acta Numerica* 7 (1998) 51–150.
- [5] R.J. Duffin and A.C. Schaefer, A class of nonharmonic Fourier series, *Trans. Amer. Math. Soc.* 72 (1952) 341–366.
- [6] E. Feig and F.A. Grünbaum, Tomographic methods in range-Doppler radar, *Inverse Problems* 2 (1986) 185–195.
- [7] E. Feig and C.A. Micchelli, L^2 synthesis by generalized ambiguity functions, in: *Multivariate Approximation*, Vol. 4, eds. C.K. Chui, W. Schempp and K. Zeller (Birkhäuser, Basel, 1989) pp. 143–156.
- [8] G. Kaiser, *A Friendly Guide to Wavelets* (Birkhäuser, Basel, 1994).
- [9] G. Kaiser, Physical wavelets and radar – a variational approach to remote-sensing, *IEEE Antennas Propag. Mag.* 38 (1996) 15–24.

- [10] E.J. Kelly and R.P. Wishner, Matched-filter theory for high-velocity targets, *IEEE Trans. Military Elect.* 9 (1965) 56–59.
- [11] A.K. Louis, P. Maass and A. Rieder, *Wavelets. Theory and Applications* (Wiley, Chichester, 1997).
- [12] P. Maass, Wideband radar: The hyp-transform, *Inverse Problems* 5 (1989) 849–857.
- [13] P. Maass, Wideband approximation and wavelet transform, in: *Proc. of the IMA*, Vol. 39, eds. F.A. Grünbaum et al. (Springer, Berlin, 1990) pp. 83–88.
- [14] H. Naparst, Radar signal choice and processing for dense target environment, Ph.D. thesis, University of California, Berkeley (1988).
- [15] H. Naparst, Dense target signal processing, *IEEE Trans. Inform. Theory* 37(2) (1991) 317–327.
- [16] L. Rebollo-Neira, A. Plastino and J. Fernandez-Rubio, Reconstruction of the joint time-delay Doppler-scale reflectivity density in a wide-band regime. A frame theory based approach, *J. Math. Phys.* 41 (2001) 5325–5341.
- [17] A.W. Rihaczek, *High Resolution Radar* (McGraw-Hill, New York, 1969).
- [18] C.H. Wilcox, The synthesis problem for radar ambiguity functions, Technical Summary Report 157, United States Army, University of Wisconsin (1960).